Performance Analysis of Reduced Switch Hybrid Cascaded Multilevel Inverter with PSO-based PI Controller during Load Variations

M.Izzat Nordin
Faculty Electrical & Electronics Engineering Technology, Universiti Malaysia Pahang Al-Sultan Abdullah

Leong Ying Foo
Faculty Electrical & Electronics Engineering Technology, Universiti Malaysia Pahang Al-Sultan Abdullah

M.H.A. Ab Malek
Tokyo Electric Power Services Co. Ltd (TEPSCO)

Suliana Ab Ghani
Faculty Electrical & Electronics Engineering Technology, Universiti Malaysia Pahang Al-Sultan Abdullah

他

https://doi.org/10.5109/7323363

出版情報：Proceedings of International Exchange and Innovation Conference on Engineering & Sciences (IEICES). 10, pp.874-881, 2024-10-17. International Exchange and Innovation Conference on Engineering & Sciences
バージョン：

Performance Analysis of Reduced Switch Hybrid Cascaded Multilevel Inverter with PSO-based PI Controller during Load Variations

M.Izzat Nordin[1], Leong Ying Foo[1], M.H.A. Ab Malek[2], Suliana Ab Ghani[1], N.Huda Ramlan[1],
[1]Faculty Electrical & Electronics Engineering Technology,
Universiti Malaysia Pahang Al-Sultan Abdullah, 26600 Pekan, Pahang, Malaysia.
[2]Tokyo Electric Power Services Co. Ltd (TEPSCO), 1-7-12 Shinonome, Koto City, Tokyo 135-0062, Japan.
Corresponding author email: hudaramlan@umpsa.edu.my

Abstract: *This paper presents the design and simulation of a Hybrid Multilevel Inverter (HMLI) optimized for reduced switch count and minimized total harmonic distortion (THD), while maximizing output voltage. The proposed HMLI configuration employs four voltage sources and five MOSFET switches, achieving peak-to-peak output voltage of 135V at a modulation index of 0.9. The harmonic minimization is accomplished using an LC filter and Alternate Phase Opposition Disposition (APOD) PWM technique. The performance evaluation, including analysis under no-load to full-load conditions as well as half-load to full load conditions, demonstrates that Particle Swarm Optimization-based PI (PSO-PI) controller significantly enhances system performance, maintaining nominal load output of 149.8 V with a THD of 2.23%. Under varying load conditions, the HMLI with PSO-PI controller shows a 5.23% THD and 147.58µs response time, compared to ZN-PI controller. The results demonstrate that HMLIs with PSO-PI controller offers enhanced voltage regulation, reduced harmonic distortion and rapid dynamic response during load transition.*

Keywords: Multilevel Inverter; PI Controller; Hybrid MLI; Particle Swarm Optimization; Voltage Regulation

1. INTRODUCTION

Multilevel Inverters (MLIs) represent a significant advancement in power electronics, distinguished by their superior waveform quality and efficiency compared to traditional two-level inverters. Their growing importance is evidenced by their adoption in renewable energy systems and high-power industrial drives, where their enhanced efficiency and output waveform quality are crucial [1]. Multilevel inverters (MLIs) use multiple small voltage levels to produce a stepped output voltage waveform, making them ideal for high-power and medium-voltage applications. Their advantages include reduced total harmonic distortion (THD), less strain on switches, lower rates of voltage change (dv/dt), minimized rates of current change (di/dt), and decreased electromagnetic interference (EMI)[2,3].

MLIs exhibit a wide variety of configurations, with cascaded H-bridges and hybrid structures being among the most prominent [2,4]. Recent advancements focus on reducing switch power ratings, improving harmonics performance, and minimizing electromagnetic interference for practical applications across sectors [5,6,7]. Classical MLI topologies can become costly and complex with increasing output voltage levels, necessitating advanced control strategies [2,8]. However, controlling the output voltage waveform under varying loads poses challenges. The Proportional-Integral-Derivative (PID) controller emerges as a solution, stabilizing MLI systems by continuously adjusting the control signal based on feedback to maintain stable and efficient output voltage waveforms. The proportional-integral (PI) controller is the most employed controller in industrial applications due to its straightforward design, ease of implementation, and cost-effectiveness [9]. However, tuning and coordination of multiple voltage levels in the MLI can be complex, making it difficult to maintain stability and achieve accurate voltage control. Particle Swarm Optimization (PSO) algorithm differs from genetic algorithms as it focuses on collective information sharing among particles rather than individual chromosomes. This collaborative approach enhances population optimization [10,11]. Particle Swarm Optimization (PSO) provides high-quality solutions quickly and converges more reliably, making it preferable to stochastic methods like genetic algorithms (GA) [12]. Particle Swarm Optimization (PSO) algorithm can produce high-quality solutions quickly and exhibit stable convergence attributes [13]. This study aims to design and simulate a Hybrid Multilevel Inverter (HMLI) with reduced switch count and THD, while maximizing output voltage, and to evaluate Particle Swarm Optimization Proportional-Integral (PSO-PI) controllers for performance comparison in the HMLI system.

2. METHODOLOGY

This chapter outlines the methodology for designing, simulating, and implementing the Hybrid Multilevel Inverter (HMLI) system. The approach combines qualitative and quantitative methods to investigate the proposed configuration using MATLAB/Simulink.

2.1 7-Level Hybrid Multilevel Inverter

A hybrid multilevel inverter (HMLI) combines different inverter topologies, such as neutral point clamped and cascaded H-bridge, to generate multiple voltage levels, reducing harmonic distortion and improving power quality. This design consists of four voltage sources and five unidirectional MOSFET switches, it can alternatively use a combination of three switches that allow current to flow in only one direction and two switches that permit current to travel in both directions. The simplified equations governing the output voltage levels and the number of switches is:

$$N_{level} = 2m + 1 \quad (1)$$

$$m = 2s - 1 \quad (2)$$

Where N_{level} is the number of output voltage levels, m is the total number of switches and s is the number of DC sources. Reduced switches make the circuit compact and user-friendly, and although using four DC sources to generate a 7-level MLI results in less utilization of sources, the reduction in switches benefits in lower switching losses. H-Bridge is not used, and just two switches play the role of polarity reversal. Fig. 1 below shows the 7-Level HMLI and the parameters of the system are included in Table 1.

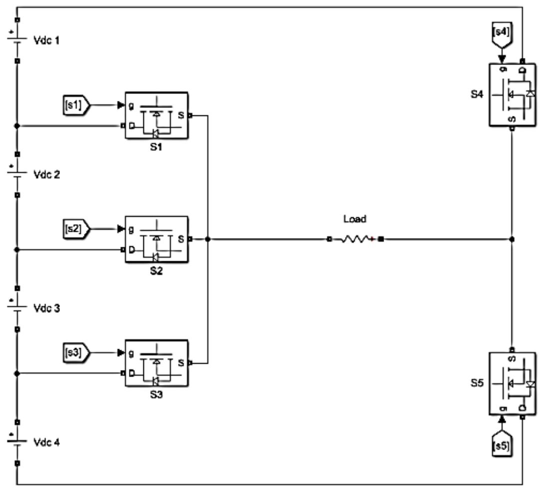

Fig. 1. Seven Level Proposed HMLI Configuration

Table 1. HMLI Parameter Design

Parameters	Value
Dc Voltage Source, V_{dc}	200V
System Frequency, f_{sys}	50Hz
Switching Frequency, f_{sw}	23.7 kHz
Sample Time, t_s	1µs
Output Voltage, V_o	135V
Resistor, R	30.375Ω
Inductor, L	3.4184mH
Capacitor, C_1	617.5nF
Ripple Capacitor, C_2	1.235µF

2.2 PWM Technique

The simulation and analysis phases of this study involved the implementation of PWM techniques, with a concentration on the Level Shift Pulse Width Modulation which is Alternate Phase Opposition Disposition Modulation (APODPWM). All carrier waveforms in the Alternate Phase Opposition Disposition PWM (APOD) have a 180-degree phase shift as each carrier waveform is 180 degrees out of phase with its adjacent carrier wave. When compared to even carrier waveforms, odd carrier waveforms are out of phase with one another.

In pulse generation, it is essential to use unidirectional switches for S1, S2, and S3 to avoid distortions in the output waveform. A reference signal is compared with a carrier signal to generate a pulse that triggers the logic gates, which then activate the switches at precise moments to create the desired waveform. For instance, switch S1 requires a pulse to achieve voltage levels of +Vdc and -3Vdc. Similarly, S2 needs to operate at +2Vdc and -2Vdc, and S3 at +3Vdc and -Vdc. Additionally, switches S5 and S4 are responsible for conducting the positive and negative half-cycles, respectively, ensuring a complete and accurate waveform.

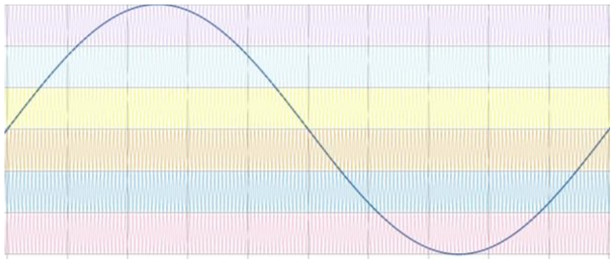

Fig. 2. APOD PWM with 90% Modulation Index

To operate the seven-stage hybrid inverter, seven switching patterns are utilised. When closed, the switches take on the values "0," and when opened, they take on the values "1". Table 2 below shows the switching scheme for 7-Level Proposed HMLI.

Table 2. Switching Scheme for 7-Level Proposed HMLI

Switching Mode	S1	S2	S3	S4	S5	Output Voltage
1	1	0	0	0	1	+3Vdc
2	0	1	0	0	1	+2Vdc
3	0	0	1	0	1	+Vdc
4	0	0	0	0	0	0
5	1	0	0	1	0	-Vdc
6	0	1	0	1	0	-2Vdc
7	0	0	1	1	0	-3Vdc

2.3 Double Loop PI Controller

A PI controller is commonly applied in inverters for its simplicity and stability, but it needs precise tuning to address issues like slow response and overshoot. To reduce harmonic distortion, a double-loop PI controller is effective. It uses an outer loop to control the output voltage and an inner loop to adjust current, enhancing efficiency and ensuring accurate voltage and phase control. Fig. 3 shows the block diagram of Double Loop PI Controller.

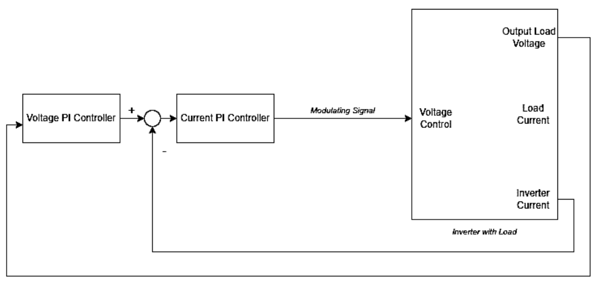

Fig. 3. Block Diagram of Double Loop PI Controller

Particularly, the voltage output at the load side is compared to a reference voltage, which acts as an input to the voltage controller. Simultaneously, the current on the inverter side is determined and compared to a reference current produced by the voltage controller, which provides input to the current controller. This dual feedback technique allows for separate and exact control over numerous variables, resulting in a more responsive and accurate system.

2.3.1 PI Parameter Tuning for Double Loop Controller

In designing a double loop controller for a voltage and current control system, adjusting the PI variables is essential to achieve peak performance. The double-loop controller system features an inner loop for current regulation and an outer loop for maintaining voltage levels across the load. Initial tuning of proportional (*Kp*) and integral gains (*Ki*) is typically done using methods like Particle Swarm Optimization (PSO) iteratively adjusts these gains to minimize errors for more precise tuning. PSO approach produce control signals for the inverter's Pulse Width Modulation (PWM) system, which converts these signals into voltage pulses that directly affect the inverter's output. Fig. 4 below shows the block diagram of the inverter system with the PSO approach.

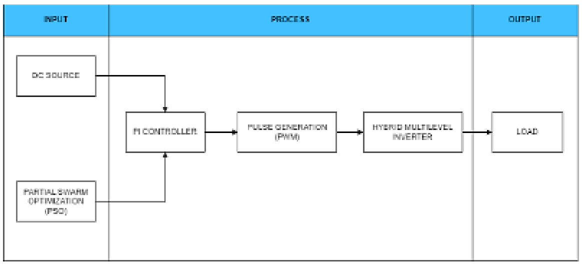

Fig. 4. Block Diagram of Inverter System

2.3.2 Zieger-Nichols Heuristic

Ziegler-Nichols method is heuristic, relying on identifying critical points in the step response curve. By drawing a tangent line at the inflection point where the slope is highest, process parameters can be derived, forming the basis for calculating controller parameters. Although the Ziegler-Nichols tuning approach may not provide optimal performance or disturbance tolerance, it offers guidance on configuring gain levels for a relatively decent control system. In this method, gain terms are expressed in terms of Ku (with Kp factored outside the brackets), and the oscillation period Tu (with Ti and Td defined in terms of Tu). The procedures for tuning using Ziegler-Nichols are as follows:

- Set Kp and Ki to zero.
- Increase Kp from 0 until the system begins to oscillate at a specific frequency.
- Calculate the value of $Ku = Kp$ and the period of the oscillation as Tu.
- Determine the different gain factors using the algorithm.

$$u(t) = K_p\, e(t) + K_1 \int e(t)dt \qquad (3)$$

Table 3. Ziegler-Nichols Tuning Method

Control Type	*K*	*Ti*	*Td*	*Tp*
P	0.5*Ku*	0	-	*Tu*
PI	0.4*Ku*	0.8*Tu*	-	1.4*Tu*
PID	0.6*Ku*	0.5*Tu*	0.125*Tu*	0.85*Tu*

2.3.3 Particle Swarm Optimization

The PSO-PI tuner utilizes a machine learning technique inspired by the natural behaviours of bird flocks or fish schools, known as Particle Swarm Optimization (PSO), to intelligently control system parameters. In this method, MATLAB is used to script the determination of the proportional (*Kp*) and integral (*Ki*) gains for both voltage and current controllers. Fig. 5 below shows the flowchart of PSO Algorithm.

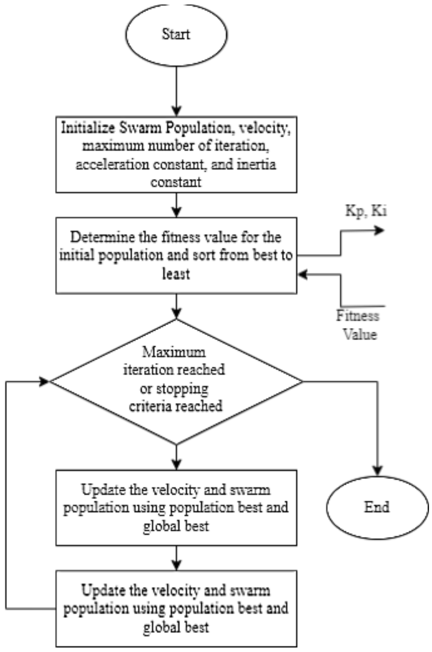

Fig. 5. Flowchart of PSO Algorithm

To integrate this approach with an inverter model in MATLAB, the transfer function of the inverter must be defined within the script as the objective function. This setup allows for the optimization of controller settings to achieve desired performance characteristics.

$$VoltageCont(s) = V_{kp} + \frac{V_{ki}}{s} \qquad (4)$$

$$CurrentCont(s) = I_{kp} + \frac{I_{ki}}{s} \qquad (5)$$

The variables in the PSO algorithm are Vkp and Vki, which represent the proportional and integral gains for the voltage controller, and Ikp and Iki, which represent the proportional and integral gains for the current controller. These parameters are optimised within the algorithm to provide the best possible performance for the controllers. Fig. 6 below shows an inverter equivalent circuit.

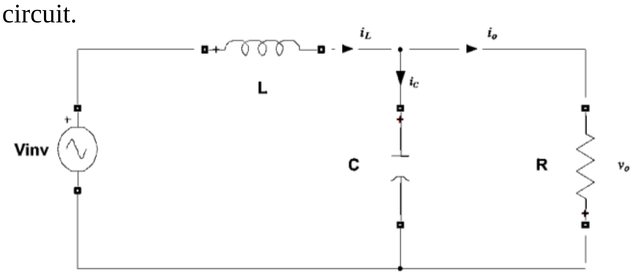

Fig. 6. Inverter Equivalent Circuit

The equivalent circuit shown in the figure shows various multilevel inverter structures and power switch bridge configurations, as well as the use of bipolar or unipolar modulation for a single-phase inverter. Represented by the inverter's filter, this equivalent circuit can be further modelled using a block diagram. In this model, the output voltage, inductor voltage, and inverter input are labelled as V_O, V_L, V_{in} respectively. The transfer function of the filter, referred to as *First Loop (s)*, is provided in the equation below.

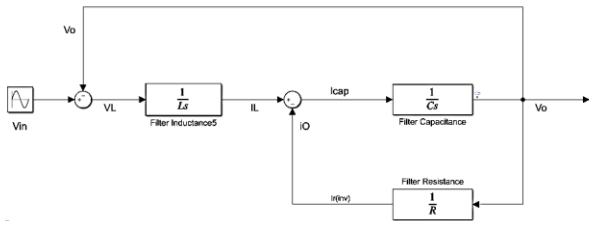

Fig. 7. Inverter Filter Model Block Diagram

$$FirstLoop(s) = \frac{V_O(s)}{V_L(s)} = \frac{R}{RLCs^2 + Ls^2} \quad (6)$$

The voltage control error will be adjusted to create a reference signal for the inductor current. This signal is then compared to iL in the current controller. The resulting control signal from these controllers is used for PWM control of the inverter, determining the switching actions of the power switches.

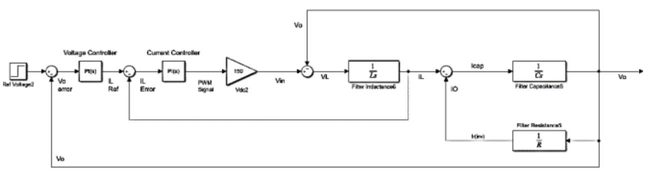

Fig. 8. Double Loop Closed Loop System

Following the reduction of the first loop's block diagram, the second loop appears, encompassing the current controller's transfer function with a feedback link by the filter inductance, Ls. The transfer function for this closed-loop system, which includes the feedback element, is defined as follows:

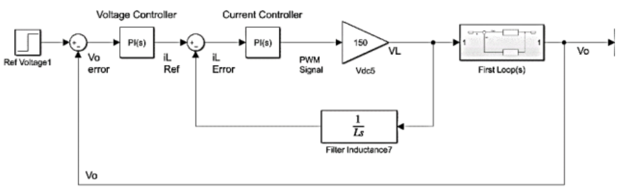

Fig. 9. Second Looping Closed Loop System

$$SecondLoop(s) = \frac{C(s)}{R(s)} = \frac{G(s)}{1 + G(s)H(s)} \quad (7)$$

$$SecondLoop(s) = \frac{CurrentCont(s)}{1 + CurrentCont(s) * 1/Ls}$$

The third loop is also present, and its forward path comprises the combined transfer functions of the first and second loops, as well as a feedback loop consisting of a resistor, R.

$$ThirdLoop(s) = \frac{C(s)}{R(s)} = \frac{G(s)}{1 + G(s)H(s)} \quad (8)$$

$$ThirdLoop(s) = \frac{FirstLoop(s) * SecondLoop(s)}{1 + FirstLoop(s) * SecondLoop(s) * 1/R}$$

Furthermore, the whole transfer function of the overall inverter system is obtained by integrating the forward gain from the third loop with the voltage controller, as well as a unity feedback loop from the output. The equation below presents the transfer function for this configuration.

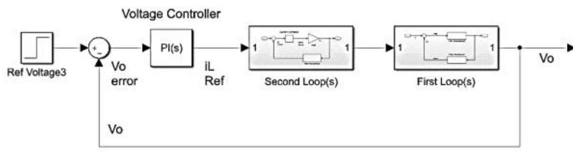

Fig. 10. Block Diagram of Inverter System

$$Inverter\ System(s) = \frac{C(s)}{R(s)} = \frac{G(s)}{1 + G(s)H(s)} \quad (9)$$

$$Inverter\ System(s) = \frac{ThirdLoop(s) * VoltageCont(s)}{1 + ThirdLoop(s) * VoltageCont(s)}$$

3. SIMULATION & RESULTS ANALYSIS

The proposed seven-level Hybrid Multilevel Inverter (HMLI) is analysed in two parts: transient response and voltage output. Each section analyses the efficiency of a distinct approaches for setting PI gain values: the Particle Swarm Optimisation method (PSO-PI). This methods are evaluated under a variety of load conditions, such as nominal load, transitions from no load to full load, and half load to full load.

3.1 Transient Analysis

Transient analysis is required for determining the stability and performance of an inverter system under changing conditions. It analyses the way the system responds to unanticipated shift such as load changes. The study focuses on the capability of the system to respond efficiently to disturbances and recover to a stable state. Key characteristics evaluated involve overshoot, rise time and settling time, which represents the time required for the output to stabilize within a predefined tolerance; also, steady-state error.

3.1.1 Step Response Analysis

Step response analysis evaluates a control system's reaction to a rapid input change. By applying a step input, critical parameters such as rise time, settling time, overshoot, and steady-state error can be measured. These metrics provide insights into the system's dynamic behavior, stability, and performance, essential for tuning controllers and optimizing systems. The discussion below covers step response analysis for the Hybrid Multilevel Inverter without a controller, with a ZN-PI controller, and with a PSO-PI controller. Fig.11 shows the step response of the inverter system when implementing PSO-PI controller.

Table 4 provides a comparative analysis of step response data, illustrating key performance metrics like rise time, settling time, peak overshoot, and steady-state error for different system configurations or controllers.

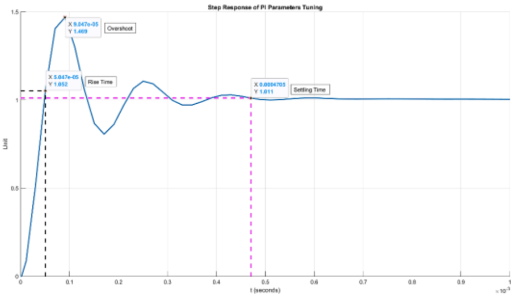

Fig. 11. Step Response of PSO-PI Controller.

Table 4. Step Response Comparison

Controller	Overshoot (%)	Rise Time (μs)	Settling Time (μs)
No Controller	0	210.50	310.50
ZN-PI	42.20	50.47	370.50
PSO-PI	45.30	50.47	470.50

Table 4 shows that PI controllers increase overshoot, with PSO-PI controllers having the highest, surpassing limits. Fig. 11 indicates the PSO-PI response has the same rise time as the ZN-PI but a higher settling time, leading to faster response and more overshoot with many oscillations before stabilizing. Despite these oscillations, the system remains stable by normal criteria, but low stability may prevent reaching the desired setpoint.

3.1.2 No Load to Full Load

The no-load-to-full-load condition was used to analyze the transition. The change occurs when the breaker trips, allowing current to flow through the 30.375Ω load. In this case, the switching can be identified as a disturbance to the steady state because it transitions from no load to full load. The transient response study focuses on the duration it requires to attain a steady state under full load conditions using a sinusoidal signal.

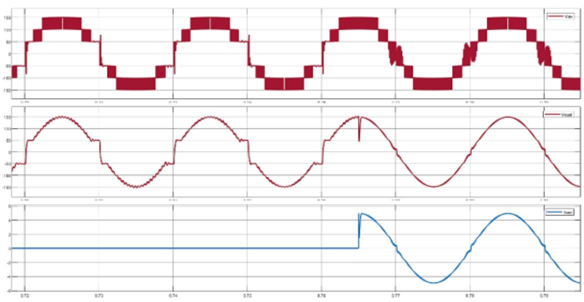

Fig. 12. Output Waveform No Load to Full Load with PSO-PI Controller

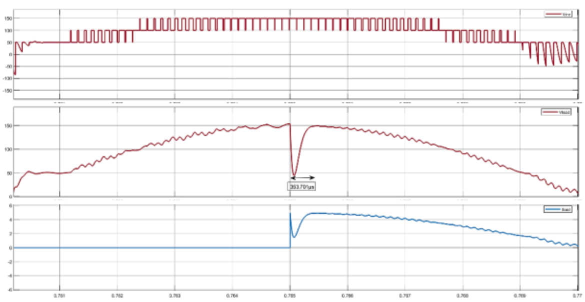

Fig. 13. Switching Duration with PSO-PI Controller

Fig. 12 and Fig. 13 above shows the inverter transitioning from no load to full load with a PSO-PI controller, stabilizing the output waveform to a near-perfect sinusoidal wave. The PSO-PI controller adjusts parameters to maintain this output, restoring stability within 353.701μs despite the rapid load increase, as shown in Table 5.

Table 5. No Load to Full Load Comparison

Controller	Overshoot (%)	Rise Time (μs)	Settling Time (μs)
No Controller	0	381.086	381.086
ZN-PI	0	358.587	358.587
PSO-PI	0	353.701	353.701

The efficiency of advanced control systems in optimizing inverter responsiveness and stability is evident in the performance comparisons. Without a controller, the system exhibits a rise and settling time of 381.086μs with no overshoot. The PSO-PI controller significantly improves performance, reducing these times to 353.701μs with zero overshoot, outperforming the ZN-PI controller's 358.587μs. The ZN-PI controller reduces both times to 358.587μs with zero overshoot. The PSO-PI controller achieves the best performance with the lowest rise time of 353.701μs and zero overshoot, indicating the fastest and most stable response among the controllers compared during this condition.

3.1.3 Half Load to Full Load

This study examines the transition from half to full load, where the full load resistance 60.75Ω is double the half load resistance 30.375Ω. At 0.765s, a breaker trips, shifting the current flow and introducing potential disturbances. Effective management of this transition is crucial for system stability. The transient response analysis focuses on the time required to return to steady state under full load with a sinusoidal signal.

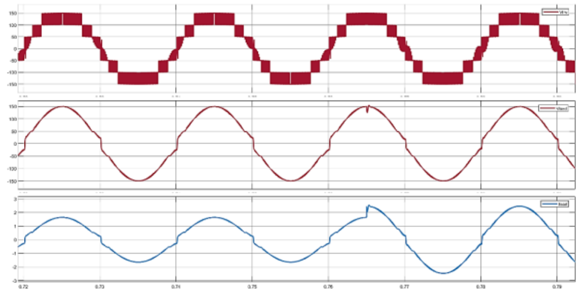

Fig. 14. Output Waveform Half Load to Full Load with PSO-PI Controller

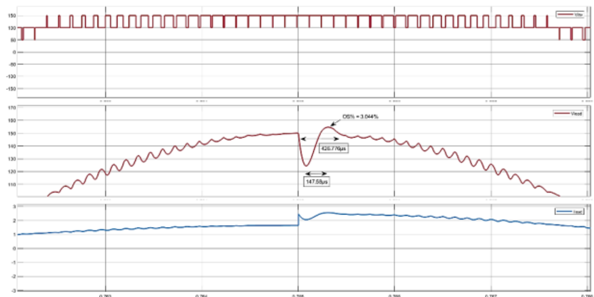

Fig. 15. Switching Duration with PSO-PI Controller

Fig. 14 and Fig. 15 above shows the inverter transitioning from half load to full load with a PSO-PI controller. During the transition from half load to full load, the system exhibits its fastest recovery time, taking 426.776µs to return to a sinusoidal state as shown in Table 6. This notably outperforms scenarios without controllers or with ZN-PI controller.

Table 6. Half Load to Full Load Comparison

Controller	Overshoot (%)	Rise Time (µs)	Settling Time (µs)
No Controller	2.62	248.065	248.065
ZN-PI	2.58	158.549	404.716
PSO-PI	3.044	147.58	426.776

Table 6 compares the performance of different controllers from half load to full load. No-Controller setup has an overshoot of 2.62%, with a rise time and settling time of 248.065µs. ZN-PI controller slightly reduces overshoot to 2.58%, with a much lower rise time of 158.549µs but a higher settling time of 404.716µs. PSO-PI controller has the highest overshoot at 3.044%, the lowest rise time at 147.58µs, and the highest settling time at 426.776µs, indicating a trade-off between rise time and overshoot.

Regarding settling time, PSO-PI controllers show higher values, indicating a system are slower than the system with no controller. This is due to the high overshoot in the output waveform caused by the transient response. Overall, the PSO-PI controller proves to be the fastest in providing feedback, which is crucial in this load condition since transient response during switching are significant for all controller types.

3.2 Output Voltage Analysis

This study analyses the proposed HMLI's output voltage waveform, focusing on peak-to-peak voltage and Total Harmonic Distortion (THD). The peak-to-peak voltage reflects the voltage range after inversion, related to power transmission capacity. THD analysis measures deviations from the ideal sinusoidal waveform.

3.2.1 Nominal Load

The nominal load condition refers to evaluation with a constant, linear resistive load. For this analysis, a 30.3750Ω resistor has been connected to the low-pass filter's output. Fig. 16 below shows PSO-PI performance during nominal load condition.

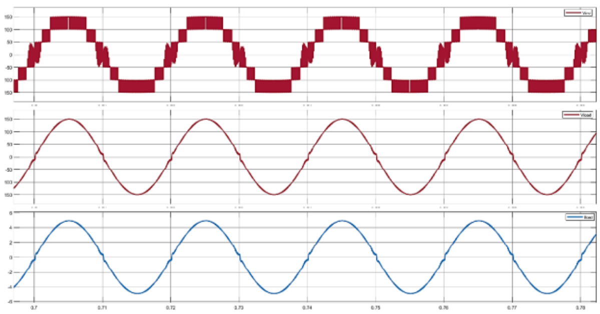

Fig. 16. Output Waveform Nominal Load with PSO-PI Controller

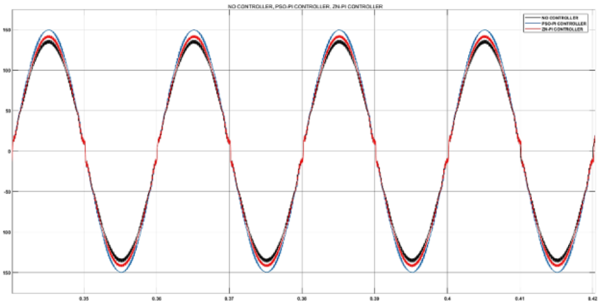

Fig. 17. Output Waveform Nominal Load Comparison between NC,ZN-PI and PSO-PI

Fig. 17 shows the comparison of output voltage waveforms under nominal load conditions for the proposed hybrid multilevel inverter using different controllers: no controller (NC), ZN-PI and PSO-PI. During nominal load, the PSO-PI controller achieved the highest peak-to-peak voltage compared to the No-Controller (NC) and ZN-PI, as shown in Table 7.

Table 7. Nominal Load Voltage Output Comparison

Controller	Peak to Peak Voltage (V)	THD (%)
No Controller	137.4	2.7
ZN-PI	143.1	2.5
PSO-PI	149.8	2.23

Table 7 compares the peak-to-peak voltage and Total Harmonic Distortion (THD) during nominal load for different controllers. NC setup has a peak-to-peak voltage of 137.4V with a THD of 2.7%. ZN-PI controller improves these values to 143.1V and a THD of 2.5%. PSO-PI controller achieves the highest peak-to-peak voltage at 149.8V and the lowest THD at 2.23%, indicating superior performance in voltage output and harmonic distortion reduction. Fig. 18 below illustrates the graphical comparison of output voltage and THD percentages among NC and PSO-PI during nominal load conditions.

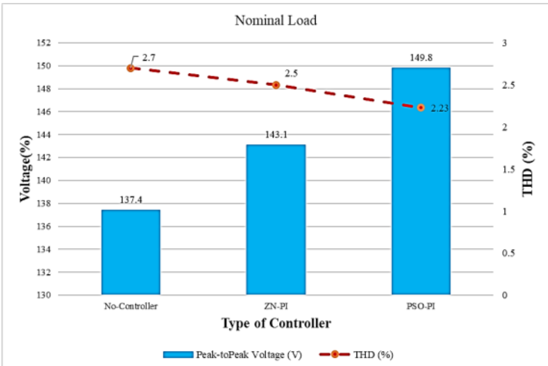

Fig. 18. Output Voltage and THD (%) Comparison during Nominal Load

Based on Table 7 and Fig. 18, both the PSO-PI controller and ZN-PI controller scenarios achieve THD below 5%, meeting IEEE 519 recommendations. The implementation of the PSO-PI controller in the system results in a decrease in THD, while also achieving the highest output voltage. This indicates the PSO-PI controller's superior performance in suppressing harmonic distortion and maintaining peak-to-peak voltage. It also effectively optimizes PI parameters, producing high-quality output voltage waveforms while meeting specified criteria, outperforming the no controller setup.

3.2.2 No Load to Full Load

Throughout this transition from no load to full load, the peak-to-peak voltage is expected to stay constant since the full load rating and circuit configuration largely remain unchanged. The analysis primarily focuses on the Total Harmonic Distortion (THD) percentage during load transition.

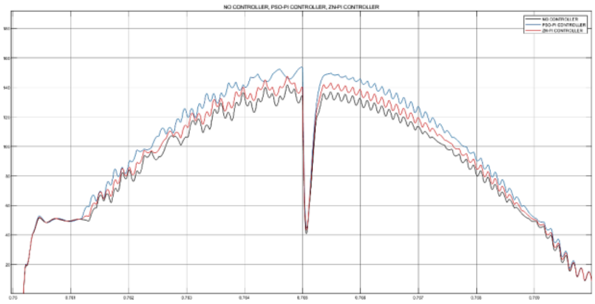

Fig. 19. Output Waveform No Load to Full Load Comparison between PSO-PI Controller and No Controller

Table 8. No Load to Full Load Voltage Output Data Comparison

Controller	Peak to Peak Voltage (V)	THD (%)
No Controller	134.2	10.23
ZN-PI	140.2	9.64
PSO-PI	153.5	9.03

Fig. 19 shows a change from no load to full load at 0.765s. All controllers, including NC, ZN-PI and PSO-PI, manage to minimize transient during load variation. Table 7 compares the performance of NC, ZN-PI, and PSO-PI controllers from no load to full load with the PSO-PI controller achieves the highest peak-to-peak voltage 153.5V and the lowest THD 9.03%, indicating superior voltage regulation and power quality. Based on Fig.19, the PSO-PI controller could maintain a high output voltage under varying load conditions suggests better overall performance in managing load variations compared to the other controllers. Fig. 20 illustrates the comparison of output voltage and Total Harmonic Distortion (THD) during no load to full load conditions.

Based on Fig. 20, PSO-PI controller, when compared to No-Controller and ZN-PI configurations, is hypothesized to achieve superior voltage regulation with the highest peak-to-peak voltage 153.5V and the lowest THD at 9.03%, indicating that its improved voltage quality comes at the cost of greater voltage fluctuations during transitions.

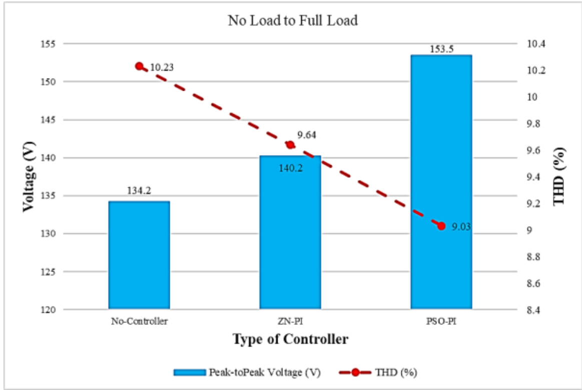

Fig. 20. Output Voltage and THD (%) Comparison during No Load to Full Load

3.2.3 Half Load to Full Load

It is expected that the peak-to-peak voltage will remain consistent during this transition from half load to full load, ensuring the stability of the voltage levels despite the change in load.

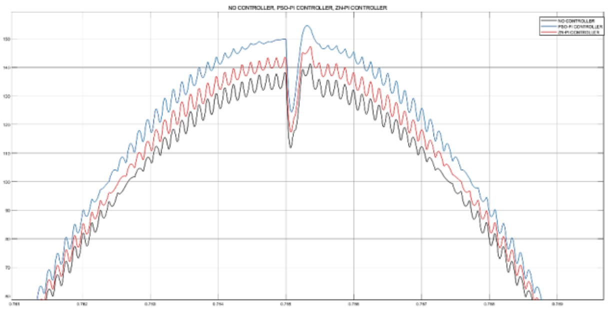

Fig. 21. Output Waveform Half Load to Full Load Comparison between PSO-PI Controller and No Controller

The comparison between NC, ZN-PI and PSO-PI during the transition from half load to full load occurring within 0.765s is shown in Fig. 21. Based on Fig. 21, it shows that the voltage drop decreased when the system was implemented with a ZN-PI controller and a PSO-PI controller. Substantial THD is similarly observed across all three controllers, as outlined in Table 9.

Table 9. Half Load to Full Load Voltage Output Data Comparison

Controller	Peak to Peak Voltage (V)	THD (%)
No Controller	137.7	6.07
ZN-PI	143.6	5.67
PSO-PI	149.9	5.20

The analysis of output voltage and Total Harmonic Distortion (THD) during the transition from half load to full load highlights the superior performance of the PSO-PI controller. Fig. 22 shows that the PSO-PI controller achieves the highest output voltage 149.9V and the lowest Total Harmonic Distortion (THD) of 5.2%, demonstrating superior voltage stability.

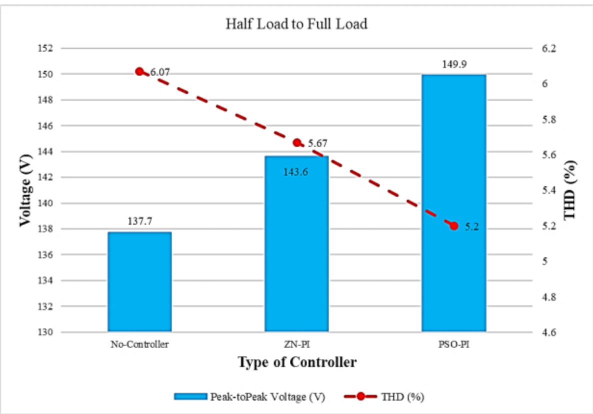

Fig. 22. Output Voltage and THD (%) Comparison during Half Load to Full Load

4. CONCLUSION

The use of reduced-switch Hybrid Multilevel Inverters (HMLIs) offers significant cost savings in power electronic systems by requiring fewer switching devices and gate drive circuits, thereby lowering installation, maintenance, and operational costs. This study evaluates HMLI performance under various load conditions with different controllers. The PSO-PI controller outperforms the system without a controller, demonstrating superior transient response and voltage regulation. For instance, under nominal load, it achieves 149.8V with 2.23% THD, and Under varying load conditions, the HMLI with PSO-PI controller shows a 5.20% THD and 147.58µs response time, compared to ZN-PI controller. Future research will explore hybrid control techniques to enhance transient response and voltage drop during load variations, along with comprehensive grid integration studies to optimize HMLIs' impact on grid functionality and reliability, thus promoting a more sustainable and resilient energy future.

5. REFERENCES

[1] Sane, Sharvari, Et Al. "Multilevel Inverter Solution For Present Inverter In Local Trains In Mumbai." International Journal of Electrical and Electronics Engineering Research (IJEEER) ISSN (P, Vol. 4, No. 2, Apr. 2014, Pp. 21–32.

[2] S. Kakar, S. B. M. Ayob, A. Iqbal, N. M. Nordin, M. Saad Bin Arif, And S. Gore, "New Asymmetrical Modular Multilevel Inverter Topology with Reduced Number of Switches," IEEE Access, Vol. 9, Pp. 27627–27637, 2021, Doi: 10.1109/Access.2021.3057554.

[3] H. P. Vemuganti, D. Sreenivasarao, S. K. Ganjikunta, H. M. Suryawanshi, and H. Abu-Rub, "A Survey on Reduced Switch Count Multilevel Inverters," IEEE Open Journal of The Industrial Electronics Society, Vol. 2, Pp. 80–111, 2021, Doi: 10.1109/Ojies.2021.3050214.

[4] S. Debnath and M. Saeedifard, "A New Hybrid Modular Multilevel Converter for Grid Connection of Large Wind Turbines," IEEE Trans Sustain Energy, Vol. 4, No. 4, Pp. 1051–1064, 2013, Doi: 10.1109/Tste.2013.2266280.

[5] M. Murugesan, R. Pari, R. Sivakumar, And S. Sivaranjani, "Different Types of Multilevel Inverter Topologies-A Technical Review," International Journal of Advanced Engineering Technology Int J Adv Eng Tech, Pp. 149–155.

[6] Bhatnagar, Jainy, And Vikramaditya Dave. "A Comparative Study of Different Topologies of Multilevel Inverters." International Journal of Electrical and Electronics Engineering Research (IJEEER) ISSN P, Vol. 9, No. 1, Jan. 2017.

[7] N. Susheela and P. Satish Kumar, "Performance Evaluation Of Multicarrier Based Techniques For Single Phase Hybrid Multilevel Inverter Using Reduced Switches," Indonesian Journal Of Electrical Engineering And Computer Science, Vol. 7, No. 3, Pp. 676–686, Sep. 2017, Doi: 10.11591/Ijeecs.V7.I3.Pp676-686.

[8] S. Bandil, S. Kushwaha, S. Soni, And Y. Rathode, "7-Level Cascaded H-Bridge Multilevel Inverter," International Research Journal of Engineering and Technology, 2020.

[9] K. S. Rao and R. Mishra, "Comparative Study Of P, PI and PID Controller for Speed Control Of VSI-Fed Induction Motor," 2014.

[10] X. Rao and X. Yan, "Particle Swarm Optimization Algorithm Based on Information Sharing in Industry 4.0," Wirel Commun Mob Comput, Vol. 2022, 2022, Doi: 10.1155/2022/4328185.

[11] K. Matsumoto and C. Ikuta, "Particle Swarm Optimization with Coupled Map Lattice," 2020 International Symposium on Nonlinear Theory and Its Applications, NOLTA2020, Nov. 2020.

[12] Y. Bekakra and D. Ben Attous, "Optimal Tuning of Pi Controller Using PSO Optimization for Indirect Power Control for DFIG Based Wind Turbine With MPPT," International Journal of System Assurance Engineering and Management, Vol. 5, No. 3, Pp. 219–229, 2014, Doi: 10.1007/S13198-013-0150-0.

[13] N. Guru, A. Prusty, S. Pani, K. Nanda, And A. K. Barisal, "Intelligent Control Based Level Shifted PWM Multilevel Inverter," In 2022 International Conference on Intelligent Controller and Computing for Smart Power, ICJCCSP 2022, Institute of Electrical and Electronics Engineers Inc., 2022. Doi: 10.1109/Iciccsp53532.2022.9862462.